12 月 December
2019, 62(12): 1359 – 1368
昆 虫 学 报
ACTA ENTOMOLOGICA SINICA
http://www.insect.org.cn
doi: 10.16380/j.kcxb.2019.12.002

Role of *DaFOXO*1 in the regulation of superoxide dismutase gene expression and developmental duration of summer diapause pupae of *Delia antiqua* (Diptera: Anthomyiidae)

PENG Zhu-Qing, HAO You-Jin*
(College of Life Sciences, Chongqing Normal University, Chongqing 401331, China)

Abstract: 【Aim】 The aim of this study is to investigate the role of *DaFOXO*1 in the regulation of superoxide dismutase (SOD) gene expression and the developmental duration of summer diapause pupae of the onion fly, *Delia antiqua*. 【Methods】 Genes encoding copper-zinc superoxide dismutase (DaCu/Zn SOD) and manganese superoxide dismutase (DaMn SOD), downstream genes of *DaFOXO*1, were identified from the transcriptome data of *D. antiqua*. The features of amino acid sequences, subcellular localization and phylogeny of DaCu/Zn SOD and DaMn SOD of *D. antiqua* were analyzed by using bioinformatic tools. The expression patterns of *DaFOXO*1, *DaCu/Zn SOD*, and *DaMn SOD* at different developmental stages of summer diapause pupae of *D. antiqua* were determined by qRT-PCR. The effect of knocking down *DaFOXO*1 by RNAi on the expressions of *DaCu/Zn SOD* and *DaMn SOD*, the activity variations of DaCu/Zn SOD and DaMn SOD and the developmental duration of summer diapause pupae of *D. antiqua* were further analyzed. 【Results】 The open reading frame (ORF) of *DaCu/Zn SOD* (GenBank accession no. KR072551) of *D. antiqua* is 459 bp in length and encodes 153 amino acids with a predicted molecular weight (MW) of 22.4 kD and an ioselectric point (pI) of 6.44, which belongs to a cytoplasmic Cu/Zn SOD. The ORF of *DaMn SOD* (GenBank accession no. KR072549) is 648 bp in length and encodes 216 amino acids with a predicted MW of 24.4 kD and a pI of 8.85, which belongs to mitochondrial Mn SOD. Amino acid sequence alignment revealed that DaCu/Zn SOD and DaMn SOD share 75% – 94% identity with their homologues from other 10 species of Diptera, and contain typical SOD family domains. Phylogenetic analysis showed that they formed a robust phylogenetic branch with their homologues in *Lucilia cuprina*. qRT-PCR analysis revealed that the expression levels of *DaFOXO*1 were higher at the pre-diapause and post-diapause stages, but lower at the diapause stage. Higher expression of *DaCu/Zn* occurred at the diapause stage and post-diapause stage. However, the highest expression level of *DaMn SOD* was detected at the pre-diapause stage and diapause stage, and followed by at post-diapause stage. Knockdown of *DaFOXO*1 by RNAi significantly decreased the expression levels of *DaCu/Zn SOD* and *DaMn SOD*, and the activities of their corresponding enzymes, leading to a significantly extended duration of summer diapause pupae. 【Conclusion】 The results suggest that DaCu/Zn SOD and DaMn SOD are important members of FOXO1 signaling network, and DaFOXO1 plays an important role in the regulation of the duration of summer diapause pupae of *D. antiqua*.

Key words: *Delia antiqua*; *FOXO*1; diapause; superoxide dismutase; pupal duration; RNAi

1 INTRODUCTION

The onion fly, *Delia antiqua*, is an economical important pest of *Allium* plants throughout the northern hemisphere and can enter into summer or winter diapause to cope with unfavorable seasons (Hao *et al.*, 2016). Insect diapause is a precisely regulated state that consists of several successive phases: induction, preparation, initiation, maintenance, termination and post-diapause quiescence (Kostál, 2006). As an important adaption strategy, insect diapause is thought to play important roles in preserving population and maintaining the population growth (Hao *et al.*, 2016), which is characterized by arrested growth or development, decreased metabolism, increased stress resistance and extended lifespan (Xu *et al.*, 2018). Once diapause terminates, the development resumes at the post-diapause stage if conditions are favorable. However, clear molecular mechanisms of diapause termination are unknown, especially the down-stream mechanisms involved in diapause hormone and

基金项目: 重庆市科学技术委员会项目(cstc2016jcyjA0152)
作者简介: 彭竹清, 女, 1994 年 10 月生, 重庆云阳人, 硕士研究生, 研究方向为生物化学与分子生物学, E-mail: 982248720@qq.com
* 通讯作者 Corresponding author, E-mail: haoyoujin@hotmail.com
收稿日期 Received: 2019-07-21; 接受日期 Accepted: 2019-09-09

ecdysone, and up-stream factors of termination. Therefore, deeper understanding of the molecular mechanisms governing diapause termination is of high importance in the improvement of pest management and also can give answers to fundamental questions such as aging and lifespan.

Previous studies revealed that many genes responsible for lifespan extension are conserved across phyla. Among them, insulin/fork head transcription factor (INS/FOXO) signaling is a key regulator controlling the lifespan of diapause fly *Drosophila melanogaster* (Giannakou and Partridge, 2007), mosquito *Culex pipiens* (Sim and Denlinger, 2008; Sim *et al.*, 2015), cotton bollworm *Helicoverpa armigera* (Zhang *et al.*, 2017), and the dauer nematode *Caenorhabditis elegans* (Lee *et al.*, 2001). During the whole diapause process, the INS/FOXO signaling pathway is suppressed and regulates the expression of some genes associated with cold tolerance, UV resistance and reactive oxygen species (ROS) resistance (McElwee *et al.*, 2003; Murphy *et al.*, 2003; Oh *et al.*, 2006; Gershman *et al.*, 2007).

Several theories were put forward to address the underlying mechanisms of aging, including ROS detoxification mechanism, which is one of the well-known mechanisms for maintaining the homeostasis and lifespan extension. ROS includes O_2^-, H_2O_2, and $OH^·$, which can be generated as a byproduct of the normal metabolism. Excessive ROS can damage proteins, lipids and nucleic acids, and cause mitochondrial dysfunction, as well as serious effects on the integrity of cell membranes. To balance ROS levels, insects possess an effective antioxidant defense system that consists of enzymatic components, such as superoxide dismutase (SOD), catalase (CAT) and peroxidase (POX), and non-enzymatic components, such as reduced glutathione and vitamin C (Jena *et al.*, 2013). Among these antioxidant enzymes, SOD is the first and the most important enzyme against ROS. This protein family contains three major isoforms: cytoplasmic Cu/Zn SOD, extracellular Cu/Zn SOD, and mitochondrial Mn SOD. They differ in the metal binding, cellular location, structure and primary functions. However, the physiological level of ROS may act as messenger molecules in a variety of biological processes including health-extending (Brys *et al.*, 2010) and health-promoting (Ristow *et al.*, 2009). In dauer state of *C. elegans*, an equivalent stage of insect diapause, ROS can extend the lifespan by inactivating the insulin signaling pathway (Zarse *et al.*, 2012). A recent study reported that the lifespan of *H. armigera* diapause pupae was increased by the physical level of ROS (Zhang *et al.*, 2017). These results indicate that insulin and ROS play important roles in diapause regulation. However, it is still not well-known how ROS plays a dual function and what signaling pathway is activated by ROS to extend lifespan of diapause insects.

In our previous study, the expression levels of fork head transcription factor 1 gene (*DaFOXO*1) and its putative downstream target gene *DaCu/Zn SOD* and *DaMn SOD* were differentially expressed during the diapause process of *D. antiqua* (Hao *et al.*, 2016; Ren *et al.*, 2018; Xu *et al.*, 2018). Furthermore, the termination of diapause pupae of *D. antiqua* has not yet been investigated at the molecular level. Therefore, we asked whether FOXO-SOD signal is involved in the regulation of developmental duration of summer diapause pupae. To this end, downstream genes encoding DaCu/Zn SOD and DaMn SOD of *DaFOXO*1 of *D. antiqua* were identified from the transcriptome, and characterized by bioinformatic analysis. Moreover, the effect of knocking down *DaFOXO*1 by RNAi on the expression of *DaCu/Zn SOD* and *DaMn SOD*, their enzymatic activity changes and diapause duration were analyzed. Our results will be helpful for better understanding how the INS/FOXO signaling pathway regulates the pupal duration of onion fly and other diapause insects.

2 MATERIALS AND METHODS

2.1 Test insects

A colony of *D. antiqua* was established in our laboratory (Xu *et al.*, 2018). Adults were maintained on artificial diet at 20 ± 0.5℃ and 50% – 70% relative humidity with a photoperiod of 16L: 8D. To obtain summer diapause pupae, adults and larvae were kept at 25 ± 0.5℃ and 50% – 70% relative humidity with a photoperiod of 16L: 8D. The pupation day was set as day 0 (D0). Pupae in pre-diapause (D0.5 and D1.5), diapause (D2, D4 and D8) and post-diapause stages (D14 and D20) were collected for survey of developmental stage-specific gene expression. Based on gene expression pattern, pupae at late diapause stage (D10) were selected for subsequent analysis.

2.2 Identification of superoxide dismutase genes and bioinformatics analysis

To identify genes encoding superoxide dismutases, BLASTP searching was performed against the transcriptome data of onion fly using *D. melanogaster* Mn SOD (GenBank accession no. NP476925) and Cu/Zn SOD (GenBank accession

no. NP476735) as queries (Hao *et al.*, 2016). The complete open reading frames (ORFs) were predicted using the ORF Finder (https://www.ncbi.nlm.nih.gov/orffinder/). Conserved domains were predicted by the SMART (http://smart.embl-heidelberg.de/) and CD search (https://www.ncbi.nlm.nih.gov/Structure/cdd/wrpsb.cgi). The protein molecular weight (MW) and the isoelectric point (pI) were predicted by Expasy (https://web.expasy.org/compute_pi/). Signal peptide and subcellular localization were analyzed by SignalP3.0 (http://www.cbs.dtu.dk/services/SignalP/) and WolfPsort (https://wolfpsort.hgc.jp/), respectively. To know the phylogenic relationship of DaMn SOD or DaCu/Zn SOD with their homologues in closely related insect species, amino acid sequences were aligned using MAFFT (http://mafft.cbrc.jp/alignment/server/), and ambiguous regions were removed by Gblock (http://molevol.cmima.csic.es/castresana/Gblocks_server.html). The best-fit evolutionary model was predicted by Modeltest (Posada, 2006). The maximum-likelihood phylogenetic trees were constructed based on the model of WAG + G for both DaMn SOD and DaCu/Zn SOD with MEGA X (Kumar *et al.*, 2018). The bootstrap consensus trees were inferred from 1 000 replicates.

2.3 RNA extraction and cDNA synthesis

Total RNA was extracted from one pupa of *D. antiqua* from Section 2.1 using the TRIzol Reagent (Invitrogen, USA) and treated with DNase to remove contaminated DNA. The quantity and quality were determined with a NanoDrop ND-1000 (Thermo Fisher Scientific) and gel electrophoresis, respectively. The first-stranded cDNA was synthesized in a 20 μL reaction mixture using the RevertAid™ First Strand cDNA Synthesis Kit (Thermo, USA), including 3 μg RNA, 1 μL oligo d(T)18 primer (50 ng/μL) and incubated at 65℃ for 5 min. Then, 5 μL 5 × reaction buffer, 1 μL Riolock™ RNase Inhibitor (20 U/μL), 2 μL dNTP Mix (10 mmol/each), 1 μL RevertAid™ M-MuLV transcriptase (20 U/μL) were added. The total reaction mix was incubated at 25℃ for 5 min, 42℃ for 60 min, 70℃ for 5 min and stored at −20℃ for further use.

2.4 qRT-PCR detection of gene expression patterns

qRT-PCR was performed to detect the expression levels of *DaFOXO*1, *DaCu/Zn SOD* and *DaMn SOD* in *D. antiqua* at different developmental stages described as in Section 2.1 in a 20 μL system, including 1 μL cDNA (obtained from Section 2.3), 10 μL 2 × SybrGreen Mix, 0.8 μL each forward and reverse primer (10 μmol/L each) and 7.4 μL ddH_2O. The PCR conditions were as follows: 94℃ for 3 min; then 40 cycles of 94℃ for 20 s, 58℃ for 20 s, 72℃ for 20 s; and a final extension at 72℃ for 3 min. The relative expression levels were calculated by the $2^{-\Delta\Delta Ct}$ method (Livak and Schmittgen, 2001) using *GAPDH* as the reference gene. All samples were analyzed in three biological and three technical replicates. Gene specific primers were designed based on the sequences obtained in this study and the sequence of *DaFOXO*1 deposited in GenBank database (GenBank accession no. MG813258). All primer sequences were listed in Table 1.

Table 1 Primers used in this study

Gene	GenBank accession no.	Forward primer sequence (5′−3′)	Reverse primer sequence (5′−3′)	Purpose
*DaFOXO*1	MG813258	ACGCTTAATGGTCCGCTGTC	TTTGGATAGGCGGGTGACAT	qRT-PCR
EGFP	U55762	GCCACAAGTTCAGCGTGTC	CTCGATGTTGTGGCGGATCT	
DaCu/Zn SOD	KR072551	CGTCATGTTGGTGATTTGGGT	TCTTCGAATCGGGATGGGTT	
DaMn SOD	KR072549	GTTGGGGTTGGTTGGGCTAT	TCAACATAAGAGGGGCGCAA	
GAPDH	NP525108	ACGTGGTGCTGCCCAAAACATCATT	GGCGGACAGTCAAATCAACAAGG	
*DaFOXO*1	MG813258	CGTTCATTAACCTGCACCT	GCCTGCAATTGATTTATTTG	RNAi
*DaFOXO*1	MG813258	TAATACGACTCACTATAGGC GCGTTCATTAACCTGCACCT	TAATACGACTCACTATAGGC GGCCTGCAATTGATTTATTTG	
EGFP	U55762	TAATACGACTCACTATAGGC GGCCACAAGTTCAGCGTGTC	TAATACGACTCACTATAGGCG CTCGATGTTGTGGCGGATCT	

2.5 Preparation of double-stranded RNA

A 596 bp fragment of *DaFOXO*1 was amplified from a previously constructed vector pMD-19T-*DaFOXO*1 using the primer set DaFOXO1-2 (Table 1) as described by Xu *et al.* (2018). Template preparation for double-stranded RNA (dsRNA) synthesis was conducted in a 15 μL system containing 1 μL DNA template (596 bp fragment), 1.5 μL reaction buffer, 1.2 μL Mg^{2+} (2.5 mmol/L), 1.2 μL dNTPs (10 mmol/L each), 0.6 μL forward and reverse primer (10 mmol/L each) (DaFOXO1-3), 0.1 μL Taq polymerase and 8.8 μL H_2O. The PCR program was as follows: denaturation at 94℃ for 3 min; 35 cycles of 94℃ for 30 s, 56℃ for 30 s, and 72℃ for 1 min; and a final extension at 72℃ for 3 min. The PCR product was

checked in a 1.0% agarose gel, and then purified for dsRNA preparation. The dsRNA synthesis was conducted in a 20 μL reaction mixture, including 10 μL RiboMAX™ Express T7 2 × buffer, 1 μL above PCR product, 7 μL H_2O and 2 μL enzyme mix. The mixture was incubated at 37℃ for 12 h, and then 1 μL RNase-free DNase (1 U/μL) was added to remove DNA, followed by the incubation at 95℃ for 5 min, 72℃ for 10 min, 60℃ for 10 min, 50℃ for 8 min and 37℃ for 10 min. The ds*EGFP* was also prepared and used as the positive control as described previously (Xu *et al.*, 2018). The resulting synthesized ds*DaFOXO*1 or ds*EGFP* was precipitated with LiCl solution, suspended in RNase-free water and quantified by a NanoDrop ND-1000 (Thermo Fisher Scientific). The concentration was quantified and diluted to a final concentration of 1 μg/μL for later use.

2.6 Effect of knocking down *DaFOXO*1 by RNAi on the expression levels of *DaMn SOD* and *DaCu/Zn SOD*

Three hundred and sixty summer diapause (D10) pupae were divided into three groups randomly (120 pupae each). Based on the dose optimization, each pupa was injected with 1 μg ds*DaFOXO*1 (treatment group) or ds*EGFP* (positive control) via the abdomen region. After the injection, all pupae were transferred to the original rearing condition (see Section 2.1). The pupae without any treatment were used as the negative control (CK). The sampling time was set at 0, 4, 8, 12, 16, 20, 24 and 36 h after injection and three pupae at each sampling point for each group were collected for gene expression pattern analysis by qRT-PCR as described in Section 2.4.

2.7 Effect of knocking down *DaFOXO*1 by RNAi on SOD activities

RNAi treated pupa from Section 2.6 (3 pupae for each sampling point) was homogenized in 0.5 mL physical salt solution, centrifuged at 4℃ 3 000 r/min for 5 min and the supernatant was used for protein quantification and enzymatic activity assays. The total protein content was determined using a commercial kit (Comin Biotech, Suzhou). The activities of DaMn SOD and DaCu/Zn SOD were determined using the Total SOD (T-SOD) detecting Kit (Nanjing Jiancheng Bio. Inst., Nanjing) following the manufacturer's instructions. The DaCu/Zn SOD activity was obtained by subtracting the activity of DaMn SOD with inhibitor addition. The SOD activity was expressed in unit (U) per microgram total protein.

2.8 Effect of knocking down *DaFOXO*1 by RNAi on the pupal eclosion

To investigate the effect of knocking down *DaFOXO*1 by RNAi on the pupal eclosion, 90 pupae for each group from Section 2.6 were selected for the eclosion experiment. Newly eclosed flies were recorded daily and the eclosion curve for adult emergence was plotted with Excel 2010.

2.9 Statistical analysis

All data were presented as means ± *SD* of three biological and three technical replicates except the pupal eclosion experiment. One-way analysis of variance (ANOVA) was performed for time-course expression pattern analysis and followed by a Duncan's test. Significant differences among data from three groups at the same sampling time were determined using a Student's *t*-test. All statistical analyses were performed using SPSS19.0 (SPSS, Inc., Chicago, IL, USA). The statistical difference was considered as significant at $P \leqslant 0.05$ and extremely significant at $P \leqslant 0.01$.

3 RESULTS

3.1 Gene identification, characterization and phylogenetic analysis

In this study, *DaMn SOD* (GenBank accession no. KR072549) and *DaCu/Zn SOD* (GenBank accession no. KR072551) were identified based on the transcriptome data. The ORF of *DaCu/Zn SOD* is 459 bp in length, coding a protein of 153 amino acids with a predicted MW of 22.4 kD and a pI of 6.44. Subcellular localization prediction revealed that DaCu/Zn SOD is a cytoplasmic protein. Similarity analysis showed that DaCu/Zn SOD shares 94% amino acid sequence identity with LcCu/Zn SOD (GenBank accession no. XP023303945) of *Lucilla cuprina*, 91% identity with MdCu/Zn SOD (GenBank accession no. NP001295981) of *Musca domestica* and 88% identity with ScCu/Zn SOD (GenBank accession no. XP013106323) of *Stomoxys calcitrans*. Multiple sequence alignment revealed that DaCu/Zn SOD contains the conserved domain of Cu/Zn SOD family (a.a. 22 – 176, E = 1e – 49) (Fig. 1: A). Cu^{2+}-binding sites (H^{45}, H^{47}, H^{62} and H^{119}) and Zn^{2+}-binding sites (H^{62}, H^{70}, H^{79}, and D^{82}) are also conserved (Fig. 1: A). The phylogenetic tree showed that DaCu/Zn SOD was phylogentically clustered with LcCu/Zn SOD of *L. cuprina* (Fig. 1: B).

The ORF of DaMn SOD is 648 bp in length, encoding a 216-amino-acid protein with a predicted molecular mass of 24.4 kD and a pI of 8.85. Subcellular localization results showed that DaMn

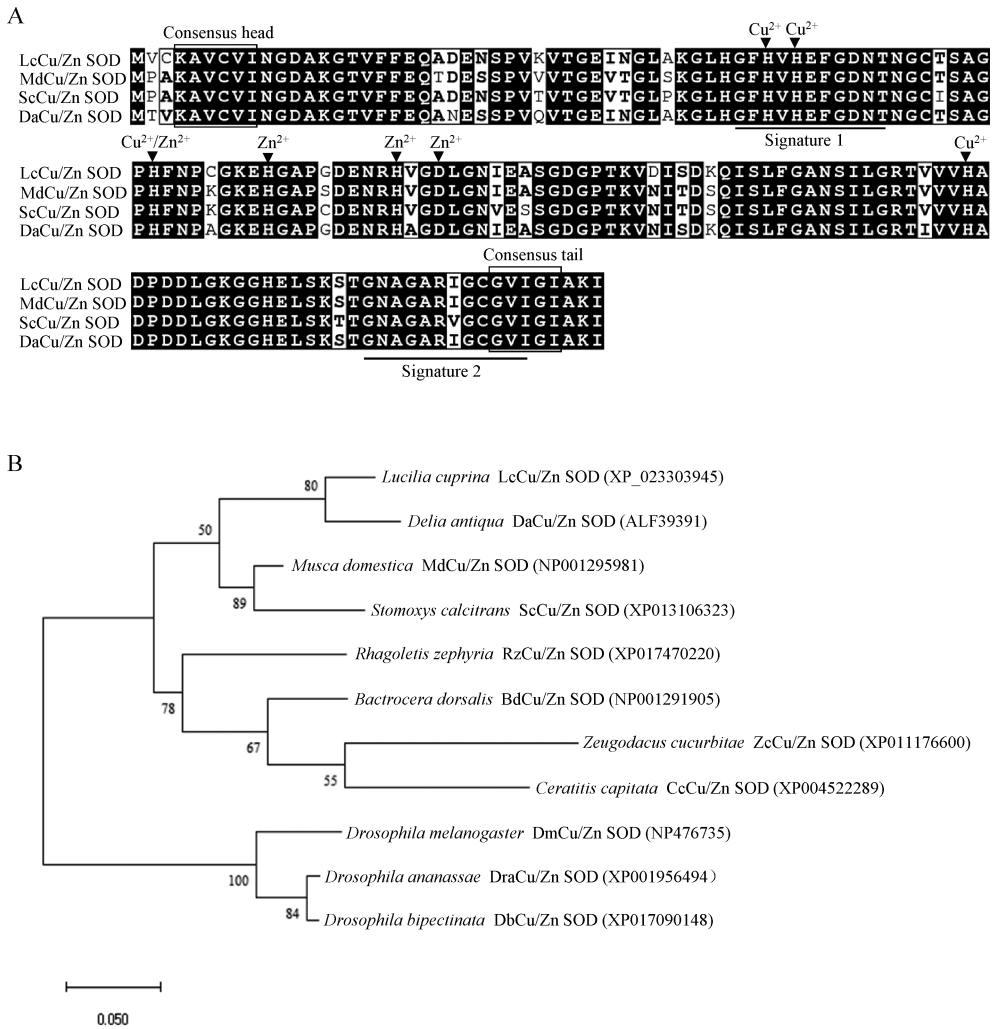

Fig. 1　Multiple sequence alignment (A) and phylogenetic tree (B) of DaCu/Zn SOD of *Delia antiqua* with its homologues from other 10 species of Diptera by maximum likelihood method

In Fig. A, the consensus head and tail were boxed, the active sites responsible for Cu^{2+}- or Zn^{2+}-binding sites were marked with inverted triangles, and the signatures of Cu/Zn SOD family were underlined. In Fig. B, the phylogenetic tree was constructed under the best evolutionary model WAG + G. Bootstrap values from 1 000 replicates were shown on each branch. The scale bar represents the substitution per amino acid site.

SOD is localized in the mitochondria. It shares 90% amino acid sequence identity with mitochondrial MdMn SOD (GenBank accession no. NP001273816) of *M. dometica* and 92% identity with mitochondrial LcMn SOD (GenBank accession no. XP023307201) of *L. cuprina*. DaMn SOD contains an N-terminal domain (a. a. 19 – 100, E = 7. 3e – 34) and a C-terminal domain (a. a 104 – 211, E = 9e – 37) (Fig. 2: A). In addition, DaMn SOD contains a typical Mn SOD signature (DVWEHAYY) and four Mn^{2+}-binding sites (H^{44}, H^{89}, D^{177} and H^{181}). The phylogenetic analysis revealed that DaMn SOD was grouped with Mn SOD of *L. cuprina*, *M. domestica* and *S. calcitrans* (Fig. 2: B).

3. 2　Developmental expression analysis of *DaFOXO*1, *DaCu/Zn SOD* and *DaMn SOD* in summer diapause pupae

To gain insights into the importance of FOXO-SOD signal in summer diapause pupae, gene expression patterns in different developmental stages of *D. antiqua* were determined by qRT-PCR. The results showed that the transcription level of *DaFOXO*1 was suppressed at the diapause stage (D2 – D8) when compared with those at the pre-diapause stage (D0. 5 – D1. 5), but the highest expression level occurred at the post-diapause stage (D20) (Fig. 3: A). Higher expression levels of *DaCu/Zn SOD* was detected at the diapause stage (D2) and post-diapause stage (D20) (Fig. 3: B). However, no clear expression pattern was found for *DaCu/Zn SOD*. The highest expression level of *DaMn SOD* was found at the pre-diapause stage (D1. 5) and diapause stage (D4), then followed by the post-diapause stage (D20) (Fig. 3: C).

3. 3　Effect of knocking down *DaFOXO*1 by RNAi on the expression of *DaCu/Zn SOD* and *DaMn SOD*

The results showed that the transcription levels

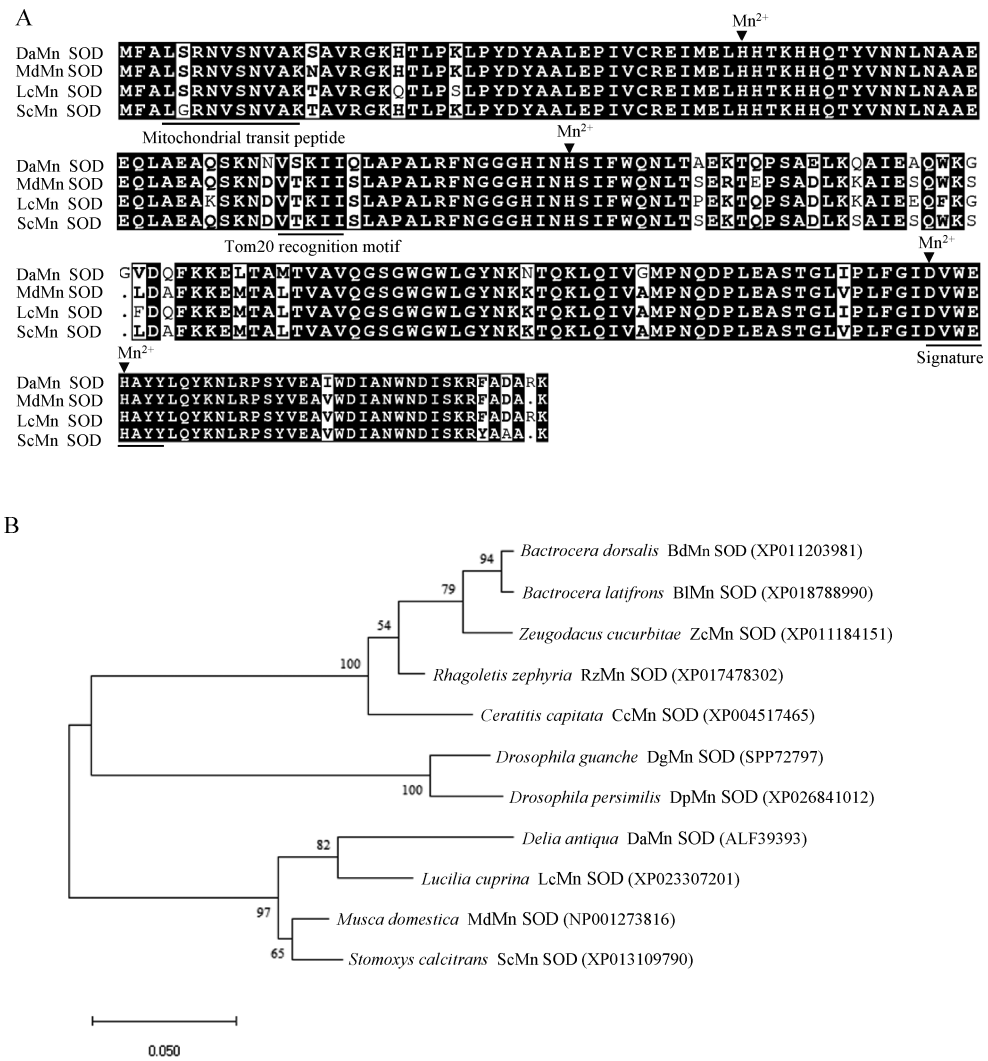

Fig. 2 Multiple sequence alignment (A) and phylogenetic tree (B) of DaMn SOD of *Delia antiqua* and its homologues from other 10 species of Diptera by maximum likelihood method

In Fig. A, the mitochondrial transit peptide, the Tom20 recognition motif and the signature of Mn SOD family were underlined, and the active sites involved in Mn^{2+}-binding were marked with inverted triangles. In Fig. B, the phylogenetic tree was constructed under the best evolutionary model WAG + G. Bootstrap values from 1 000 replicates were shown on each branch. The scale bar represents the substitution per amino acid site.

of *DaCu/Zn SOD* and *DaMn SOD* were not affected by the injection of ds*EGFP* (Fig. 4: B, C). However, the expression levels of *DaCu/Zn SOD* (Fig. 4: B) and *DaMn SOD* (Fig. 4: C) were significantly decreased after injection of ds*DaFOXO*1 (all $P < 0.05$) as compared with the negative control (CK) and the suppression effect lasted for 36 h. The minimum expression levels of *DaCu/Zn SOD* and *DaMn SOD* were observed at 8 and 4 h after injection of ds*DaFOXO*1, respectively (Fig. 4).

3.4 Effect of knocking down *DaFOXO*1 by RNAi on the activities of DaCu/Zn SOD and DaMn SOD

To investigate whether knocking down *DaFOXO*1 contributed to the reduction of SOD activities, enzymatic activity variations were measured at 0 – 36 h after the microinjection. The results showed that both activities of DaCu/Zn SOD (Fig. 5: A) and DaMn SOD (Fig. 5: B) were suppressed from 4 h after injection of ds*DaFOXO*1 when compared to the ds*EGFP*-injected group and the negative control (CK) at each sampling time point (all $P < 0.05$). The minimum activities of DaCu/Zn SOD and DaMn SOD were observed at 24 and 8 h after injection, respectively. There was a clear time lag between variations of gene expression and the corresponding enzyme activity.

3.5 Effect of knocking down *DaFOXO*1 by RNAi on the pupal duration

To elucidate the function of FOXO-SOD signal in the maintenance phase of summer diapause, the effect of knocking down *DaFOXO*1 on the pupal duration was determined based on the eclosion curve of diapause pupae. Interestingly, the length of

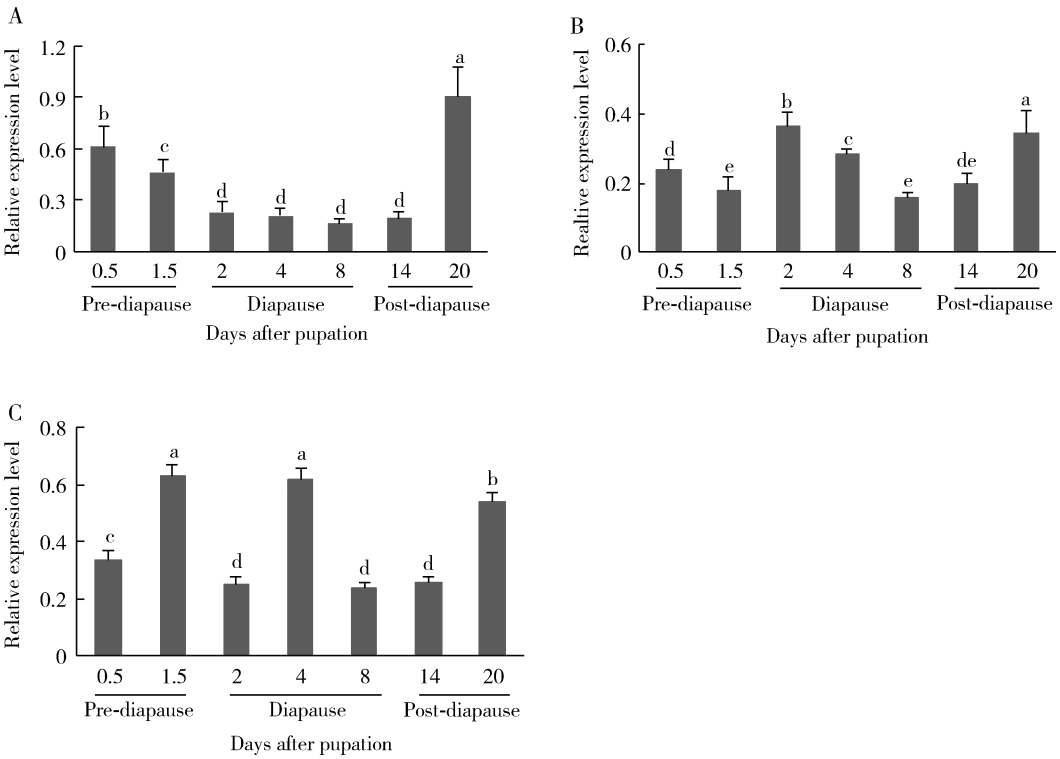

Fig. 3 Expression patterns of *DaFOXO*1 (A), *DaCu/Zn SOD* (B) and *DaMn SOD* (C) in summer diapause pupae of *Delia antiqua*

Data in the figures are mean ± *SD* of three biological replicates and three technical replicates for each sampling time point (n = 3 × 3). Gene expression levels in each group were evaluated using one-way analysis of variance (ANOVA) followed by a Duncan's multiple comparison test, and different letters above bars indicate significant difference ($P < 0.05$).

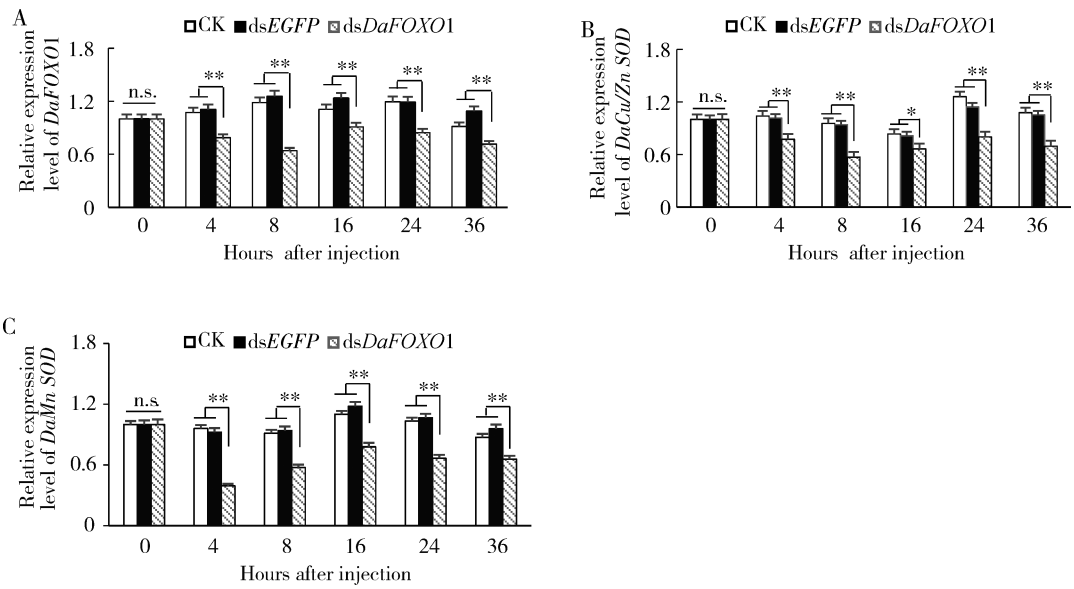

Fig. 4 Changes in relative expression levels of *DaFOXO*1 (A), *DaCu/Zn SOD* (B) and *DaMn SOD* (C) in summer diapause pupae of *Delia antiqua* after RNAi of *DaFOXO*1 detected by qRT-PCR

Pupae (D10) injected with ds*EGFP* were used as the positive control, while those without any treatment were taken as the negative control (CK). The house-keeping gene *GAPDH* was used as an internal reference gene for data normalization. The same for Figs. 5 – 6. The expression level of each gene in samples at 0 h (just after injection) was used as the calibrator. All data are mean ± *SD* of three biological replicates and three technical replicates (n = 3 × 3). Pairwise comparisons of the difference within each sampling time point were performed by the independent samples *t*-test. The difference was considered as significant when $^{*}P < 0.05$ or $^{**}P < 0.01$. n. s. represents no significant difference. The same for Fig. 5.

diapause maintenance phase was significantly extended in both ds*EGFP* and ds*DaFOXO*1 injected groups when compared with the negative control (CK). The eclosion peak was postponed about 6 and 15 d in ds*EGFP* and ds*DaFOXO*1 injected groups, respectively (Fig. 6).

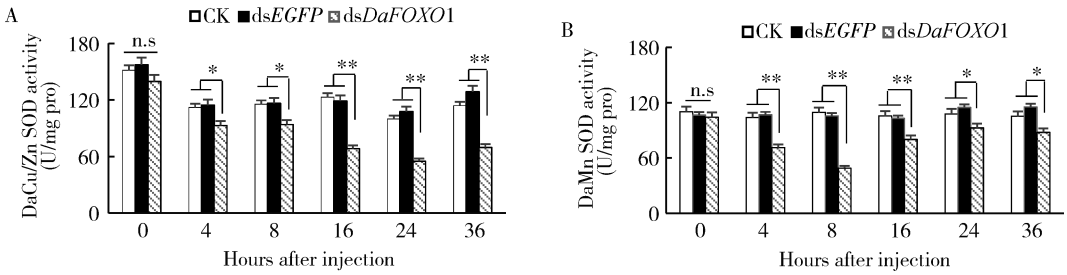

Fig. 5 Effect of knocking down *DaFOXO*1 by RNAi on the activities of DaCu/Zn SOD (A) and DaMn SOD (B) in summer diapause pupae of *Delia antiqua*

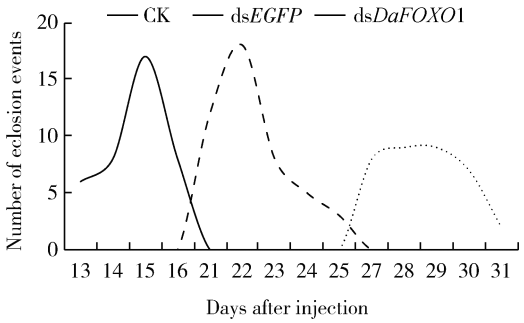

Fig. 6 Effect of knocking down *DaFOXO*1 by RNAi on the duration of summer diapause pupae of *Delia antiqua*

Pupae (D10) injected with *dsDaFOXO*1 or ds*EGFP* were kept at the same condition as the negative control (CK). Eclosion events were recorded daily over 40 d. Cumulative numbers of eclosed individuals were plotted against eclosion day using EXCEL 2010.

4 DISCUSSION

Some insects can enter into diapause, a phylogenetically regulated state of dormancy, which is characterized by the reduced metabolism, developmental arrest, and high stress tolerance. This arrest state can be terminated by favorable environmental cues (such as increasing or decreasing temperature, photoperiod change) or chemical treatment (like hormone stimuli) (Ragland *et al.*, 2011). The post-diapause development resumes if conditions are favorable, which is a very complicated process involved in various cellular events, such as protein synthesis, increased metabolism, cellular differentiation and morphological changes (Nambu *et al.*, 1997; Malarkey *et al.*, 2010). All these events occur together with large energy fluctuations and promote the accumulation of reactive oxygen species (ROS), such as hydrogen peroxide, superoxide, and hydroxyl radicals. Excessive ROS generated as by-products of metabolism can damage cellular components. However, physiological ROS level can participate in cellular signaling transduction and is essential for lifespan extension (Finkel, 2003). The involvement of ROS in cellular signaling is part of a complex, redox-based, physiological regulation. Under the normal condition, a delicate balance of intracellular oxidative stress produced by ROS is achieved by a complex system of antioxidant defense (Hao *et al.*, 2018). Superoxide dismutase enzymes (SOD) are the most important regulators of ROS level (Landis and Tower, 2005). Cu/Zn SOD functions in the cytoplasm or outer mitochondrial space, while Mn SOD functions in the inner mitochondrial space. In *Drosophila*, the mutation of *Cu/Zn SOD* or *Mn SOD* reduced lifespan (Phillips *et al.*, 1989; Kirby *et al.*, 2002), while their over-expression could extend the longevity (Parkes *et al.*, 1998; Sun *et al.*, 2004).

Previous study showed that the suppression of insulin signaling pathway gene could extend the lifespan of dauer larvae of *C. elegans* and *Drosophila* adults. It was thought that this process was regulated by the insulin-target transcription factor FOXO (Clancy *et al.*, 2001; Tatar *et al.*, 2001). Two SOD genes were identified in *C. pipiens*: a mitochondrial Mn SOD gene (*sod*-1) and a cytoplasmic Cu/Zn SOD gene (*sod*-2). However, only *sod*-2 was under the control of *FOXO* and protected ovaries of winter diapause adults (Sim and Denlinger, 2011). Why *sod*-2 is the only SOD gene involved in the diapause response of *C. pipiens* is not immediately clear. Interestingly, the expressions of orthologues of *sod*-2 and *sod*-3 were significantly up regulated and involved in lifespan regulation of *C. elegans* (Murphy *et al.*, 2003).

In our previous work, the involvement of antioxidant enzymes in redox level balance during the whole summer or winter diapause process had been determined (Hao *et al.*, 2018). Moreover, we have found that the insulin/FOXO signaling pathway plays an important role in the induction and maintaining of summer diapause in *D. antiqua* (Xu *et al.*, 2018). However, the regulatory role of FOXO-SOD signal in lifespan or summer diapause maintenance of onion fly is not known. In this study, two SOD genes were identified based on the transcriptome data and their proteins were putatively

localized in cytoplasm (DaCu/Zn SOD) and mitochondria (DaMn SOD). Their expression levels were coordinated with the expression of *DaFOXO*1. Knockdown of *DaFOXO*1 by RNA interference can suppress the expressions of *DaCu/Zn SOD* and *DaMn SOD* at both transcriptional and translational levels, but the suppression degree was different. Their different temporal and spatial expression patterns suggest that they contribute to antioxidant protection at different developmental periods. Low expression of *DaFOXO*1 and *DaSODs* can significantly extend the diapause duration of summer diapause pupae. Further examination of tissue-specific expression pattern of these genes may help explain how FOXO-SOD signal regulates the development of diapause pupae. Interestingly, diapause pupae injected with buffer with ds*EGFP* also have longer diapause duration. Although evidence indicated that water was often considered as essential for diapause complete and prerequisite for the resumption of development (Hodek, 1996), it is argued that this phenomenon is caused by water or ds*EGFP*. Similarly, when the larvae of the Colorado beetle, *Leptinotarsa decemlineata*, were fed with ds*EGFP*, the larval period was significantly extended, which causes the delay of the pupation (Guo, 2015). But the mechanism was unknown.

References

Brys K, Castelein N, Matthijssens F, Vanfleteren JR, Braeckman BP, 2010. Disruption of insulin signaling preserves bioenergetic competence of mitochondria in ageing *Caenorhabditis elegans*. *BMC Biol.*, 8: 91.

Clancy DJ, Gems D, Harshman LG, Oldham S, Stocker H, Hafen E, Leevers SJ, Partridge L, 2001. Extension of life-span by loss of CHICO, a *Drosophila* insulin receptor substrate protein. *Science*, 292(5514): 104 – 106.

Finkel T, 2003. Oxidant signals and oxidative stress. *Curr. Opin. Cell Biol.*, 15(2): 247 – 254.

Gershman B, Puig O, Hang L, Peitzsch RM, Tatar M, Garofalo RS, 2007. High-resolution dynamics of the transcriptional response to nutrition in *Drosophila*: a key role for *dFOXO*. *Physiol. Genomics*, 29(1): 24 – 34.

Giannakou ME, Partridge L, 2007. Role of insulin-like signalling in *Drosophila* lifespan. *Trends Biochem. Sci.*, 32(4): 180 – 188.

Guo WC, 2015. RNA Inteference-Mediated Knockdown of Nuclear Genes *E*75 and *HR*3 on Pupation in *Leptinotarsa decemlineata*. PhD Dissertation, Nanjing Agricultural University, Nanjing. [郭文超, 2015. RNA 干扰 *E*75 和 *HR*3 对马铃薯甲虫(*Leptinotarsa decemlineata*)化蛹的影响. 南京: 南京农业大学博士学位论文]

Hao YJ, Guo Q, Chen B, 2018. Comparisons of antioxidant properties in non-diapause, summer diapause and winter diapause pupae of *Delia antiqua* (Diptera: Anthomyiidae). *Acta Entomol. Sin.*, 61(3): 263 – 270. [郝友进, 郭强, 陈斌, 2018. 葱蝇非滞育、夏滞育和冬滞育蛹体内抗氧化酶活性的比较分析. 昆虫学报, 61(3): 263 – 270]

Hao YJ, Zhang YJ, Si FL, Fu DY, He ZB, Chen B, 2016. Insight into the possible mechanism of the summer diapause of *Delia antiqua* (Diptera: Anthomyiidae) through digital gene expression analysis. *Insect Sci.*, 23(3): 438 – 451.

Hodek I, 1996. Diapause development, diapause termination and the end of diapause. *Eur. J. Entomol.*, 93(3): 475 – 487.

Jena K, Kar PK, Babu CS, Giri S, Singh SS, Prasad BC, 2013. Comparative study of total hydroperoxides and antioxidant defense system in the Indian tropical tasar silkworm, *Antheraea mylitta*, in diapausing and non-diapausing generations. *J. Insect Sci.*, 13: 123.

Kirby K, Hu J, Hilliker AJ, Phillips JP, 2002. RNA interference-mediated silencing of *Sod*2 in *Drosophila* leads to early adult-onset mortality and elevated endogenous oxidative stress. *Proc. Natl. Acad. Sci. USA*, 99(25): 16162 – 16167.

Kostál V, 2006. Eco-physiological phases of insect diapause. *J. Insect Physiol.*, 52(2): 113 – 127.

Kumar S, Stecher G, Li M, Knyaz C, Tamura K, 2018. MEGA X: molecular evolutionary genetics analysis across computing platforms. *Mol. Biol. Evol.*, 35(6): 1547 – 1549.

Landis GN, Tower J, 2005. Superoxide dismutase evolution and life span regulation. *Mech. Ageing Dev.*, 126(3): 365 – 379.

Lee RY, Hench J, Ruvkun G, 2001. Regulation of *Caenorhabditis elegans* DAF-16 and its human ortholog *FKHRL*1 by the *daf*-2 insulin-like signaling pathway. *Curr. Biol.*, 11(24): 1950 – 1957.

Livak KJ, Schmittgen TD, 2001. Analysis of relative gene expression data using real-time quantitative PCR and the $2^{-\Delta\Delta C_T}$ method. *Methods*, 25(4): 402 – 408.

Malarkey K, Coker KJ, Sturgill TW, 2010. Ribosomal S6 kinase is activated as an early event in preemergence development of encysted embryos of *Artemia salina*. *Eur. J. Biochem.*, 251(1 – 2): 269 – 274.

McElwee J, Bubb K, Thomas JH, 2003. Transcriptional outputs of the *Caenorhabditis elegans* forkhead protein DAF-16. *Aging Cell*, 2(2): 111 – 121.

Murphy CT, McCarroll SA, Bargmann CI, Fraser A, Kamath RS, Ahringer J, Li H, Kenyon C, 2003. Genes that act downstream of *DAF*-16 to influence the lifespan of *Caenorhabditis elegans*. *Nature*, 424(6946): 277 – 283.

Nambu Z, Tanaka S, Nambu F, 1997. Gene expression of trehalase during post-dormant development of the brine shrimp, *Artemia*: comparison of the two species. *J. UOEH*, 19(4): 255 – 264.

Oh SW, Mukhopadhyay A, Dixit BL, Raha T, Green MR, Tissenbaum HA, 2006. Identification of direct *DAF*-16 targets controlling longevity, metabolism and diapause by chromatin immunoprecipitation. *Nat. Genet.*, 38(2): 251 – 257.

Parkes TL, Elia AJ, Dickinson D, Hilliker AJ, Phillips JP, Boulianne GL, 1998. Extension of *Drosophila* lifespan by overexpression of human *SOD*1 in motorneurons. *Nat. Genet.*, 19(2): 171 – 174.

Phillips JP, Campbell SD, Michaud D, Charbonneau M, Hilliker AJ, 1989. Null mutation of copper/zinc superoxide dismutase in *Drosophila* confers hypersensitivity to paraquat and reduced longevity. *Proc. Natl. Acad. Sci. USA*, 86(8): 2761 – 2765.

Posada D, 2006. Model Test Server: a web-based tool for the statistical selection of models of nucleotide substitution online. *Nucleic Acids Res.*, 34 (Web Server Issue): W700 – W703.

Ragland GJ, Egan SP, Feder JL, Berlocher SH, Hahn DA, 2011. Developmental trajectories of gene expression reveal candidates for diapause termination: a key life-history transition in the apple maggot fly *Rhagoletis pomonella*. *J. Exp. Biol.*, 214 (Pt 23): 3948 – 3959.

Ren S, Hao YJ, Chen B, Yin YP, 2018. Global transcriptome sequencing reveals molecular profiles of summer diapause induction stage of onion maggot, *Delia antiqua* (Diptera: Anthomyiidae). *Genes, Genom. Genet.*, 8(1): 207 – 217.

Ristow M, Zarse K, Oberbach A, Klöting N, Birringer M, Kiehntopf M, Stumvoll M, Kahn CR, Blüher M, 2009. Antioxidants prevent health-promoting effects of physical exercise in humans. *Proc. Natl. Acad. Sci. USA*, 106(21): 8665 – 8670.

Sim C, Denlinger DL, 2008. Insulin signaling and *FOXO* regulate the overwintering diapause of the mosquito *Culex pipiens*. *Proc. Natl. Acad. Sci. USA*, 105(18): 6777 – 6781.

Sim C, Denlinger DL, 2011. Catalase and superoxide dismutase-2 enhance survival and protect ovaries during overwintering diapause

in the mosquito *Culex pipiens*. *J. Insect Physiol.*, 57(5): 628 – 634.

Sim C, Kang DS, Kim S, Bai X, Denlinger DL, 2015. Identification of *FOXO* targets that generate diverse features of the diapause phenotype in the mosquito *Culex pipiens*. *Proc. Natl. Acad. Sci. USA*, 112(12): 3811 – 3816.

Sun J, Molitor J, Tower J, 2004. Effects of simultaneous over-expression of *Cu/ZnSOD* and *MnSOD* on *Drosophila melanogaster* life span. *Mech. Ageing Dev.*, 125(5): 341 – 349.

Tatar M, Kopelman A, Epstein D, Tu MP, Yin CM, Garofalo RS, 2001. A mutant *Drosophila* insulin receptor homolog that extends life-span and impairs neuroendocrine function. *Science*, 292 (5514): 107 – 110.

Xu YL, Peng ZQ, Si FL, Hao YJ, 2018. Characterization of fork head transcription factor 1 gene *FOXO*1 and its role in sugar and lipid metabolism in the summer prediapause pupae of *Delia antiqua* (Diptera: Anthomyiidae). *Acta Entomol. Sin.*, 61(12): 1384 – 1392. [徐燕玲, 彭竹清, 司风玲, 郝友进, 2018. 叉头转录因子 1 基因 *FOXO*1 的特征及其在葱蝇夏滞育前期蛹体内糖脂代谢中的作用. 昆虫学报, 61(12): 1384 – 1392]

Zarse K, Schmeisser S, Groth M, Priebe S, Beuster G, Kuhlow D, Guthke R, Platzer M, Kahn CR, Ristow M, 2012. Impaired insulin/IGF1 signaling extends life span by promoting mitochondrial L-proline catabolism to induce a transient ROS signal. *Cell Metab.*, 15(4): 451 – 465.

Zhang XS, Wang T, Lin XW, Denlinger DL, Xu WH, 2017. Reactive oxygen species extend insect life span using components of the insulin-signaling pathway. *Proc. Natl. Acad. Sci. USA*, 114(37): E7832 – E7840.

葱蝇夏滞育蛹体内 *DaFOXO*1 对超氧化物歧化酶基因表达及蛹发育历期的调控作用

彭竹清, 郝友进*

(重庆师范大学生命科学学院, 重庆 401331)

摘要: 【目的】本研究旨在调查葱蝇 *Delia antiqua* 夏滞育蛹体内 *DaFOXO*1 对超氧化物歧化酶(SOD)基因表达及蛹发育历期的调控作用。【方法】从葱蝇转录组数据中鉴定 *DaFOXO*1 下游铜锌超氧化物歧化酶基因 *DaCu/Zn SOD* 和锰超氧化物歧化酶基因 *DaMn SOD*;利用生物信息学工具对 DaCu/Zn SOD 和 DaMn SOD 的氨基酸序列特征、亚细胞定位和系统发育关系进行分析。通过 qRT-PCR 方法分析 *DaFOXO*1, *DaCu/Zn SOD* 和 *DaMn SOD* 基因在葱蝇夏滞育蛹不同发育阶段的表达特点;进一步分析 *DaFOXO*1 基因被干扰后,葱蝇夏滞育蛹中 *DaCu/Zn SOD* 和 *DaMn SOD* 基因的表达特点、酶活性变化及对葱蝇夏滞育蛹发育历期的影响。【结果】鉴定到的葱蝇 *DaCu/Zn SOD* (GenBank 登录号: KR072551)的开放阅读框长 459 bp,编码 153 个氨基酸,预测蛋白分子量为 22.4 kD,等电点为 6.44,属于细胞质型铜锌超氧化歧化酶; *DaMn SOD* (GenBank 登录号: KR072549)的开放阅读框长 648 bp,编码 216 个氨基酸,预测蛋白分子量为 24.4 kD,等电点为 8.85,属于线粒体型锰超氧化物歧化酶。氨基酸序列比对结果显示,DaCu/Zn SOD 和 DaMn SOD 与其他 10 种双翅目昆虫的同源蛋白有 75% ~94% 的氨基酸序列一致性,且具有典型的 SOD 家族序列特征;系统发育分析显示它们与铜绿蝇 *Lucilia cuprina* 同源蛋白形成高支持率的一支。qRT-PCR 分析表明, *DaFOXO*1 基因在滞育前期和滞育后期的表达量较高,而在滞育期的表达量低; *DaCu/Zn SOD* 基因在滞育期和滞育后期呈高表达;但 *DaMn SOD* 基因在滞育前期和滞育期的表达量最高,在滞育后期次之。干扰 *DaFOXO*1 可显著抑制 *DaCu/Zn SOD* 和 *DaMn SOD* 的基因表达及相应酶活性,并能明显延长夏滞育蛹的滞育期。【结论】结果说明,DaCu/Zn SOD 和 DaMn SOD 是 FOXO1 信号网络中的重要成员;DaFOXO1 对葱蝇夏滞育蛹蛹期有重要调控作用。

关键词: 葱蝇; *FOXO*1; 滞育; 超氧化物歧化酶; 蛹期; RNAi

中图分类号: Q966 **文献标识码:** A **文章编号:** 0454-6296(2019)12-1359-10

(责任编辑: 马丽萍)